

# DETECTING THE ONSET OF MYOCARDIAL CONTRACTION FOR ESTABLISHING INVERSE ELECTRO-MECHANICAL COUPLING IN XMR GUIDED RF ABLATION

Gerardo I. Sanchez-Ortiz<sup>1</sup> Maxime Sermesant<sup>2</sup> Raghavendra Chandrashekara<sup>1</sup>  
Kawal S. Rhode<sup>2</sup> Reza Razavi<sup>2</sup> Derek L.G. Hill<sup>2</sup> Daniel Rueckert<sup>1</sup>

<sup>1</sup> Department of Computing, Imperial College London, U.K.,  
<sup>2</sup> Guy's Hospital, King's College London, U.K.

## ABSTRACT

Radio-frequency (RF) ablation uses electrode-catheters to destroy abnormally conducting myocardial areas that lead to potentially lethal tachyarrhythmias. The procedure is normally guided with x-rays (2D), leading to errors in location and excessive radiation exposure. In order to provide pre- and intra-operative 3D MR guidance, we define a probabilistic measure of regional motion activation. Non-rigid registration of tagged MR sequences is used to track heart motion. Regional motion is also compared between different acquisitions, thus assisting in diagnosing arrhythmia, in follow up of treatment, and in determining whether ablation succeeded. We validate using an electro-mechanical model, synthetic tagged MRI, stress data on healthy volunteers, and one patient with tachyarrhythmia, before and after ablation.

## 1. INTRODUCTION

Advances in non-rigid motion tracking techniques that use tagged MR (SPAMM) now enable us to measure more subtle changes in cardiac motion patterns. One example of disease with associated changes in motion patterns are tachyarrhythmias: pathological fast heart rhythms originating either in the atria (super-ventricular) or ventricles (ventricular), often the result of abnormal paths of conduction. Radio-frequency (RF) ablation is the indicated treatment for patients with life threatening arrhythmia as well as for those on whom drug treatment is ineffective. Applying a RF current via an ablation electrode induces hyperthermia and destruction of the abnormally conducting areas. These procedures are typically carried out under x-ray (2D) guidance, leading to errors in the location of the abnormal areas as well as to excessive x-ray exposure for the patient.

One of our goals is to provide pre- and intra-operative 3D MR guidance [1] in XMR systems (combined X-ray and MRI room) by detecting the onset of regional motion and relating it to the electrical activation pattern. For this purpose in this work we define a probabilistic measure of regional

motion activation derived from a 3D motion field extracted by using non-rigid 3D registration of tagged MR image sequences. Since we address the inverse electro-mechanical problem, trying to infer time of electrical activation by extracting information from the cardiac motion, we use a cardiac atlas and an electro-mechanical model of the heart to validate these results.

The other goal of this work is to detect changes in the regional motion patterns between two different image acquisitions. The purpose being the follow up of medical treatment in general, and in particular of patients that have undergone RF ablation, aiding the identification and localisation of abnormal or changing motion patterns and helping determine whether the ablation had the desired effect of regularising cardiac contraction. We use pre- and post-intervention MR images (as well as healthy volunteers and synthetic data) in order to validate this methodology.

## 2. METHODS

### 2.1. Registration for motion tracking

We use a non-rigid registration algorithm [2] to track the motion and deformation of the heart in a sequence of 3D short- and long-axis tagged MR images. The goal of the non-rigid registration is to align each time frame of the tagged MR image sequence with the end-systolic (ES) time frame of the image sequence by maximising the normalised mutual information of both time frames. To model cardiac motion we use a free-form deformation based on cubic B-splines. The output of the registration is a continuous time varying 3D motion or vector field (see Figure 1a),  $\mathbf{F}(\mathbf{p}, t)$  where  $\mathbf{F} : \mathbb{R}^4 \rightarrow \mathbb{R}^3$  and  $\mathbf{p} \in \mathbb{R}^3$  is the space coordinate (or voxel  $(x, y, z)$  in the discrete implementation).

A manual segmentation of the myocardium at end-diastole (ED) (see Figure 1b) is used to determine the region of interest (**myo**) for the registration at time  $t = 0$ . Using  $\mathbf{F}$ , the myocardial region can then be automatically propagated over the entire cardiac cycle (as in Figure 1a).

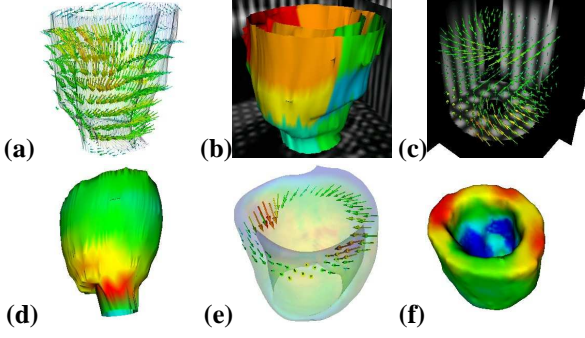


**Fig. 1.** The reconstructed motion field is shown in (a) with displacement vectors and the myocardial surface. The end-diastole myocardial surface ( $t = 0$ ) of a volunteer is shown in (b) with the subdivision in 12 segments. In (c) the synthetic tagged MR data is displayed with the recovered displacement field while the reconstructed surface in (d) is coloured with the magnitude of the difference between the normal and modified parameters. The region where the abnormal motion was produced was accurately identified and can be seen in red and yellow. The smooth cardiac atlas geometry and a slice of its motion field are shown in (e). (f) shows the isochrones (time of activation) produced with the electro-mechanical model. All colour scales go from blue to red.

## 2.2. Activation detection

The underlying assumption is that we can relate the motion derived from the images sequences to the electrical activation, in a way, addressing the inverse electro-mechanical coupling. Ideally the onset of regional contraction could be inferred from the motion field with a simple measure such as strain. However, because of the limitations imposed by noise, errors and the relatively low space and time resolution of the image acquisition and the extracted motion field, a more robust measure has to be used.

Some differential features derived from the motion field  $\mathbf{F}(\mathbf{p}, t)$  can provide an insight on whether a region of the myocardium has began contracting. We write them as the set of functions

$$F^M = F^M(\mathbf{p}, t) \text{ where } m \in M = \{D, V, E, I\}$$

and  $F^m : \mathbb{R}^4 \rightarrow \mathbb{R}$  are defined as the displacement  $F^D = \|\mathbf{F}\|$ , the velocity  $F^V = \|d\mathbf{F}/dt\|$ , a magnitude of the strain matrix  $F^E = \|E_{i,j}\|$ , and the change of strain in time  $F^I = |dF^E/dt|$ . We use a Lagrangian framework where the transform  $\mathbf{F}(\mathbf{p}, t)$  follows, at time  $t$ , the position of the 3D voxels  $\mathbf{p} \in \mathbf{myo}$  that correspond to the myocardium at time  $t = 0$ .

In order to be able to detect the regional onset of activation we need to characterise the regional motion of the heart during the cardiac cycle by measuring a regional ( $T_{ES}(\mathbf{p})$ ) and global ( $T_{ES}$ ) end-systolic times, and also the critical

times for each motion descriptor. We define

$$T_{max}^m(\mathbf{p}) = t^* \text{ such that } F^m(\mathbf{p}, t^*) \geq F^m(\mathbf{p}, t) \\ \forall t \in [0, T_{ES}(\mathbf{p})]$$

and

$$T_{min}^m(\mathbf{p}) = t^* \text{ such that } F^m(\mathbf{p}, t^*) \leq F^m(\mathbf{p}, t) \\ \forall t \in [T_{max}^m(\mathbf{p}), T_{ES}(\mathbf{p})].$$

Notice that for  $T_{min}^m$  the search interval begins at  $T_{max}^m$ , *i.e.* when the maximum value has been reached (it is the late minimum value of  $F^m$  that will help us define the end-systolic time, not those small values at the beginning of the cycle). Because the computation of these values requires a first estimate of the end-systolic time, we use as initialisation the time frame where the heart visually appears to be at end-systole. However, a short iterative process rapidly provides a better estimate for  $T_{ES}(\mathbf{p})$ .

In the case of displacement and strain, the end-systolic time is linked to their maximum values, while in the case of velocity and rate of change of strain it corresponds to their minimum values (when the heart has paused its contraction). Therefore,

$$T_{ES}^m(\mathbf{p}) = \begin{cases} T_{max}^m(\mathbf{p}) & \text{for } m \in \{D, E\} \\ T_{min}^m(\mathbf{p}) & \text{for } m \in \{V, I\} \end{cases} \quad (1)$$

and combining these times we obtain an estimate that corresponds to the regional time of end-systole:

$$T_{ES}(\mathbf{p}) = \sum_{m \in M} w_m T_{ES}^m(\mathbf{p}).$$

The weights  $w_m$  are normalised (*i.e.*  $\sum_{m \in M} w_m = 1$ ) and reflect the confidence we have on each of the differential motion descriptors  $m$ . Although at present we have assigned their values manually, a statistical measure derived from the data is being developed in order to compute them automatically. In order to obtain a global estimate for end-systolic time for each feature we integrate those values over the entire myocardium:  $T_{ES} = \int_{\mathbf{p} \in \mathbf{myo}} T_{ES}(\mathbf{p}) d\mathbf{p}$ .

Using the above equations we can now define a probabilistic measure of the activation for every voxel in the myocardium, at anytime time during the cardiac cycle:

$$A(\mathbf{p}, t) = \sum_{m \in M} w_m \int_0^t \frac{F^m(\mathbf{p}, \tau)}{\int_0^{T_{max}^m(\mathbf{p})} F^m(\mathbf{p}, \tau') d\tau'} d\tau \quad (2)$$

where we impose  $F^m(\mathbf{p}, t) = 0$  if  $t > T_{max}^m(\mathbf{p})$  in order to keep the values normalised (notice that  $F^V$  and  $F^I$  reach their maximum values before end-systole).

The value of  $A(\mathbf{p}, t)$  monotonically increases from zero to one as we expect every voxel to have been activated by

the time the motion descriptors reach the maximum value at time  $T_{max}^m(\mathbf{p})$ . In order to avoid singularities in the equation we excluded from the computation, and labelled as not active, those voxels that might remain relatively static (*i.e.* those for which  $F^m(\mathbf{p}, T_{max}^m(\mathbf{p})) \approx 0$ ).

By integrating over time we obtain an accumulated probability and we can therefore set a (percentage) threshold  $P$ , between 0 and 1, to define the time  $t_a$  at which the activation of a voxel  $\mathbf{p}$  takes place. That is, if  $A(\mathbf{p}, t_a) = P$  then  $\mathbf{p}$  becomes active for  $t = t_a$ .

In order to reduce the effect of noise in the present implementation we use a Gaussian function to smooth the computation of  $A$ , however we are working on a more appropriate Markov random field approach using spatial and time neighbours of every voxel to help deciding when does a voxel becomes active and to make  $A$  continuous over space and time. Also, the electro-mechanical model that will be described in the following section is being considered to provide a priori knowledge when applied to the specific geometry of the heart under analysis (and the more appropriate solution of inverting the equations in the model is also being explored).

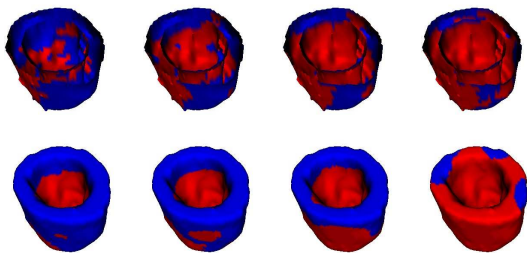


**Fig. 2.** Activation sequence on the myocardium. Each column correspond to a different time during the cardiac cycle. Blue and red show not active and active voxels, respectively. Images on the top row correspond to results obtained from the motion fields. Those on the bottom row were obtained with the electro-mechanical model. The geometry was interpolated and the top of the myocardial surface was closed to obtain higher resolution for the model.

### 2.3. Changes in regional motion patterns

The other goal of this work is to measure and detect changes in the regional motion patterns between two different image acquisitions. Some of the immediate applications are diagnosing the onset of regional diseases such as arrhythmia and ischaemia, and aiding the follow up of medical treatment, in particular, of patients that have undergone RF ablation.

In order to be able to compare different image acquisitions, a common (cylindrical) coordinate system based on the left ventricle is defined for each subject. In this man-

ner we avoid potential misregistration errors due to subject motion between scans. Using cylindrical coordinates based on the LV allows to express the non-rigid motion measurements in terms of radial, circumferential and longitudinal directions. Using this coordinate system, the myocardium is then subdivided into small meaningful regions, and the motion derived measurements for each myocardial segment computed during the cardiac cycle. In this study we use 12 segments, with 4 sections around the z-axis that roughly correspond to septum, lateral, anterior and posterior walls, and 3 sections along the z-axis, corresponding to base, middle region and apex (see Figure 1b).

The components of displacement (wall excursion), velocity and strain in this coordinate system are computed for each voxel and the values averaged for each of the myocardial segments, for all time frames during the cardiac cycle. In order to evaluate changes in the motion patterns between two data sets, a statistical measure is derived from the above combined quantities and the segment is assigned a measure of motion change and classified as having either no, small or significant changes [3].

In order to evaluate the proposed methodology in a controlled case we also implemented and modified a cardiac motion simulator for tagged MRI [4] (Figure 1c). Two sequences of synthetic tagged LV images were produced: a 'post-intervention' (normal) sequence using the standard parameters, and a 'pre-intervention' (abnormal) sequence in which the motion parameters were modified in a small region of the myocardium by moving the phase of the contraction forward in time and changing the magnitude of the motion.

## 3. RESULTS AND CONCLUSIONS

We used a **cardiac atlas** of geometry and motion generated from 3D MR images sequences of 14 volunteers to test our activation measure in a realistic but smooth and virtually noise-free data set [5] (see Figure 1e). Since we are addressing the problem of inverse electro-mechanical coupling, that is, trying to infer the time of electrical activation by extracting information from the cardiac motion images, we have also used a forward 3D **electro-mechanical model** of the heart [6] to validate our results, at this stage in a qualitative manner. The segmentation of the myocardium of a healthy volunteer at end-diastole was used as geometric input for the model. The muscle fibre orientation and the Purkinje network location were fitted to the geometry from a-priori values of the model. Figure 1f shows the isochrones values computed for this subject using the model. Figure 2 compares, in four frames of a sequence, the activation results obtained from Equation 2 and those obtained from the model (in order to simplify visual analysis we display results on the static surface corresponding to end-diastole). Promis-

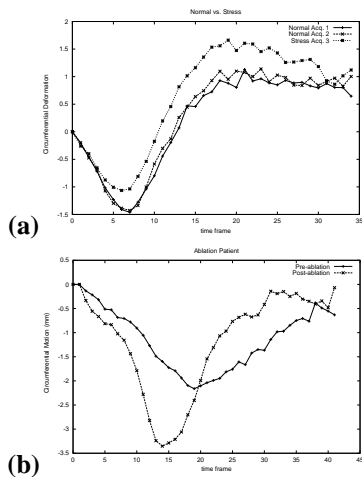


**Fig. 3.** Time plots of circumferential motion of a myocardial segment. (a) Results for the healthy volunteer show no significant changes in the motion pattern between the first two acquisitions, but a noticeable alteration when stress was induced on the subject. (b) In the case of the patient a significant change can be seen after RF ablation, when this region of the myocardium exhibits a faster and more pronounced contraction.

ing qualitative agreement can be seen on these preliminary results and we are working on further validation.

The detection of changes in motion patterns was evaluated on synthetic data as well as real MR data from six subjects. In order to test the algorithm when the ground truth is available, results on the 'pre-' and 'post-intervention' sequences of **synthetic** tagged LV images were compared in two cases, with different parameters and regions of abnormal motion (see one case in Figure 1c). In both cases these regions were accurately located. One segment showed significant changes while the rest were correctly classified as having no change (see Figure 1d).

We also acquired data from four volunteers. For each of them two separate sets of image sequences were acquired with only few minutes between the acquisitions. Since no change is expected in these pairs of image acquisitions, this allowed us to verify the **reproducibility** of the motion fields computed by the algorithm and to test the comparison method against false positive detection. The motion patterns encountered were all very similar and no region was classified as having a significant change.

With another volunteer we acquired three sets of image sequences. The first two as described above, with only few minutes between the acquisitions. The third data set was acquired few minutes after the second, but while subjecting the volunteer to **stress**. The stress was induced by placing one foot of the subject into a bucket of cold water with ice. This experiment allowed us to compare normal motion patterns with those obtained under stress, and again, to validate

the method regarding reproducibility and false positives. No segment showed a significant difference between the first two acquisitions, but when comparing normal motion to that under stress we found that three segments showed no change, four presented small but noticeable changes, and the remaining five showed a significant amount of change (see Figure 3a).

Finally, MRI data was acquired from an eight year old patient with acute super-ventricular tachyarrhythmia, before and after **RF ablation**. The image acquisition and catheter intervention were carried out with an XMR system [1]. Our results confirmed that the motion pattern changed in most parts of the myocardium (visual inspection of the reconstructed 3D surfaces and displacement vectors also showed pronounced changes in the overall contraction pattern), while the largest changes were found in five segments. Examples of the compared motion also show the corrective effect of the intervention (see Figure 3b). The methodology seems promising for the assessment of intervention results and could also be used for the detection of arrhythmia, ischaemia, regional dysfunction and follow up studies in general.

## References

- [1] K.S. Rhode, D.L.G. Hill, P.J. Edwards, J. Hipwell, D. Rueckert, G.I. Sanchez-Ortiz, S. Hegde, V. Rahunathan, and R. Razavi. Registration and tracking to integrate X-ray and MR images in an XMR facility. *IEEE Transactions on Medical Imaging*, 22(11):1369–1378, 2003.
- [2] R. Chandrashekar, R. H. Mohiaddin, and D. Rueckert. Analysis of myocardial motion in tagged MR images using non-rigid image registration. In *Proc. SPIE Medical Imaging 2002: Image Processing*, pages 1168–1179, San Diego, CA, February 2002.
- [3] G. I. Sanchez-Ortiz, R. Chandrashekar, K.S. Rhode, R. Razavi, D.L.G. Hill, and D. Rueckert. Detecting regional changes in myocardial contraction patterns using MRI. In *SPIE Medical Imaging*, San Diego, USA, Feb 2004. accepted.
- [4] E. Waks, J. L. Prince, and A. S. Douglas. Cardiac motion simulator for tagged MRI. In *IEEE Workshop on Mathematical Methods in Biomedical Image Analysis*, pages 182–191, San Francisco, CA, 1996. IEEE.
- [5] D. Perperidis, M. Lorenzo-Valdes, R. Chandrashekar, R. Mohiaddin, G. I. Sanchez-Ortiz, and D. Rueckert. Detecting regional changes in myocardial contraction patterns using MRI. In *IEEE International Symposium on Biomedical Imaging*, Arlington, USA, 2004. submitted.
- [6] M. Sermesant, K.S. Rhode, S. Hegde, G.I. Sanchez-Ortiz, D. Rueckert, P. Lambiase, C.A. Bucknall, D.L.G. Hill, and R. Razavi. Electromechanical Modelling of the Myocardium using XMR Interventional Imaging. In *Proc. of the Society for Cardiovascular Magnetic Resonance*, Barcelona, Spain, Feb 2004.